




Article

Comparison of Different Approaches to Predict the Performance of Pumps As Turbines (PATs)

Mauro Venturini * , Stefano Alvisi , Silvio Simani  and Lucrezia Manservigi

Dipartimento di Ingegneria, Università degli Studi di Ferrara, Ferrara 44121, Italy; stefano.alvisi@unife.it (S.A.); silvio.simani@unife.it (S.S.); lucrezia.manservigi@unife.it (L.M.)

* Correspondence: mauro.venturini@unife.it; Tel.: +39-0532-974878

Received: 18 March 2018; Accepted: 18 April 2018; Published: 21 April 2018



Abstract: This paper deals with the comparison of different methods which can be used for the prediction of the performance curves of pumps as turbines (PATs). The considered approaches are four, i.e., one physics-based simulation model (“white box” model), two “gray box” models, which integrate theory on turbomachines with specific data correlations, and one “black box” model. More in detail, the modeling approaches are: (1) a physics-based simulation model developed by the same authors, which includes the equations for estimating head, power, and efficiency and uses loss coefficients and specific parameters; (2) a model developed by Derakhshan and Nourbakhsh, which first predicts the best efficiency point of a PAT and then reconstructs their complete characteristic curves by means of two ad hoc equations; (3) the prediction model developed by Singh and Nestmann, which predicts the complete turbine characteristics based on pump shape and size; (4) an Evolutionary Polynomial Regression model, which represents a data-driven hybrid scheme which can be used for identifying the explicit mathematical relationship between PAT and pump curves. All approaches are applied to literature data, relying on both pump and PAT performance curves of head, power, and efficiency over the entire range of operation. The experimental data were provided by Derakhshan and Nourbakhsh for four different turbomachines, working in both pump and PAT mode with specific speed values in the range 1.53–5.82. This paper provides a quantitative assessment of the predictions made by means of the considered approaches and also analyzes consistency from a physical point of view. Advantages and drawbacks of each method are also analyzed and discussed.

Keywords: pump as turbine; pump; performance curve; simulation model; hydraulic energy

1. Introduction

In many applications, e.g., in water distribution networks [1,2], waste hydraulic energy may be available for conversion into useful electric energy. As highlighted in [3], Pumps As Turbines (PATs) couple well with low and variable power, by allowing acceptable energy production with low installation costs. In fact, pumps can be used in turbine mode by reversing flow direction [4]. An extensive review about potential benefits of PATs is documented in [5], mainly for low-capacity power generation in micro-hydropower plants as well as in water supply piping systems.

In fact, PATs can be aimed at energy saving and recovering in a water distribution network [6,7]. In [6] a novel technology, coupling a PAT and a pump has been investigated for pumping water at the end of a water supply system to a second network with higher pressure level. The paper [6] showed that (i) the system is viable in different scenarios and (ii) this strategy can replace a classic pumping system or supply the network in case the current hydraulic power is high. The work [7] compares PATs to an innovative cross-flow turbine with positive outlet pressure, defined as a Power Recovery System, which allows higher energy production and lower construction and installation costs.

The exploitation of PATs may also improve water distribution network flexibility, e.g., by changing PAT working conditions in case of pipe failure. In fact, the same authors analyzed the energy potential of four PATs to exploit the available hydraulic energy of three water distribution networks [8]. PAT effectiveness was also studied in [9] via an optimization approach, in order to also account for mechanical reliability and system flexibility at design stage.

Actually, the optimal coupling between turbomachine and available head and flow rate should be identified by also considering transient conditions, as made, e.g., by the same authors in [10–13] or by De Marchis et al. in [14].

The cost-effectiveness of PATs has also been recently analyzed. The study [15], for instance, deals with an economic and environmental analysis of PATs installation in a water distribution network. The authors evaluated the use of PATs to produce energy in a small network located in a town close to Palermo (Italy). The analysis highlighted that PATs can be feasible also from an economic point of view, but PAT installation point strongly influences energy saving effectiveness.

In any case, the key issue is the lack of a wide spectrum of PAT performance curves which could allow the choice of the most suitable machine. Therefore, establishing a correlation that defines the relationship between “pump” and “turbine” performance curves is crucial. Many studies have developed theoretical and empirical procedures for predicting PAT performance curves for the Best Efficiency Point (BEP) [16–19], while so far a general methodology is not completely defined in literature. In fact, curves are often determined experimentally case by case.

In the last year, five papers [20–24] specifically dealt with the prediction of PATs’ performance.

In [20], the laboratory results for two centrifugal pumps were presented with the aim of assessing their performance in reverse mode. Experimental data were also compared to PAT performance curves obtained by eleven models previously proposed in literature. The comparison showed that for the horizontal single-stage pump, the model of Derakhshan and Nourbakhsh [16] provides good results also outside the investigated range (flow rate numbers in [16] were lower than 0.40) for head, whereas it fails to predict power for higher flow rate numbers. Furthermore, the BEP in reverse mode can be predicted with differences generally lower than 30%.

In [21], a one-dimensional numerical code was presented, aimed at identifying the geometry and performance of a generic PAT on the basis of passage sections and losses in each section of the machine. The method was validated by using laboratory test data for six PATs. By comparing the theoretical curves to some experimental measurements on PATs working at specific speeds from 9 to 65 rpm $m^{3/4} s^{-1/2}$, the estimation error was in the range from -5.26% to 21.36% for head at BEP and in the range from -21.43% to 9.30% for efficiency at BEP. In [22] the same authors presented the results of an experimental and theoretical activity regarding twelve PATs.

The paper [23] presented a correlation aimed at predicting turbine mode operation of four centrifugal pumps. The estimation error at the BEP of the four considered PATs was in the range from -7.8% to 5.2% for head, from -13.1% to 10.8% for power, and from -2.9% to 4.2% for efficiency. The method was compared to nine previous methods found in the literature. The head and flow at BEP were precisely predicted by the method developed in [23], while all other methods had errors above 10%, in some cases 20% and even more than 80% error in other cases.

Finally, the authors of [24] presented a methodology to predict the inverse characteristic of a centrifugal pump by means of a 3-D computational fluid dynamics (CFD) code.

A strategy for relating pump to PAT behavior can rely on the solution of an estimation problem, which usually requires selecting a suitable model structure. A model structure is a parameterized family of candidate models, within which the search for a model is conducted [25]. An estimation approach exploits prior knowledge and physical insight about the system, especially when selecting the model structure. It is customary to color-code—in shades of gray—the model structure according to what type of prior knowledge has been used [26]. Therefore, white box descriptions are exploited when a model is perfectly known, i.e., it has been possible to construct it entirely from prior knowledge and physical insight. Gray box models can be used when some physical insight is available, but several

parameters remain to be determined from observed data. In this case, it is useful to consider two subcases. The physical modelling can be built on physical grounds, which has a certain number of parameters to be estimated from data. This could, e.g., be a state–space model of given order and structure [26]. On the other hand, in the semiphysical modelling, a physical insight is firstly used to suggest certain nonlinear combinations of measured data signal. These new signals are then subjected to model structures of black box character. Finally, black box models are employed if no physical insight is available or used, but the chosen model structure belongs to families that are known to have good flexibility and have been successful in the past [26]. These descriptions can rely, e.g., on linear regression models, fuzzy prototypes, wavelets, neural networks, and nonparametric models [26,27]. Each of these approaches has its own characteristics, benefits, and limitations. Before making a decision about the most suitable modeling methodology, it is necessary to survey the whole system and availability of system data, characteristics, and performance. It is also advisable to evaluate which methodology is more compatible with research expectations.

In this framework, this work deals with the comparison of different approaches to be used for the prediction of the performance curves of pumps as turbines (PATs). The considered methodologies are four, i.e., one physics-based simulation model (“white box” model), two “gray box” models, which include both theory on turbomachines and specific data correlations, as well as one “black box”. All modeling approaches are applied to literature data, regarding both pump and PAT performance curves of head, power, and efficiency over the entire range of operation of four pumps with specific speed values in the range 1.53–5.82.

Advantages and drawbacks of each approach are also analyzed and discussed. In fact, as discussed in [16], even though many approaches were proposed to identify the BEP of PATs, no single approach accurately predicts the experimental behavior for the complete range of specific speeds.

This paper is organized as follows. The simulation models for PAT operation are presented in Section 2; pump and PAT performance curves, derived from experimental data available in literature, are reported in Section 3; the reliability of the predictions of all models is presented and discussed in Section 4; finally, conclusions and guidelines about the advantages and drawbacks of each approach are provided.

2. Modeling Approaches

2.1. Physics-Based Model

The equations implemented in the physics-based (PB) simulation model developed by the authors in [28] are expressed in the form reported in [29] and allow the estimation of head, power, and efficiency of a PAT. By considering the PAT’s reverse flow, the theoretical head transferred from the fluid to the runner is smaller than actual head H_T between inlet and exhaust nozzles because of hydraulic losses Z , as shown in Equation (1):

$$H_T = \frac{1}{g} \left(u_2 c_{2m} \cot \alpha_2 - u_1^2 + u_1 c_{1m} \cot \beta_1 \right) + Z_E + Z_{La} + Z_{Le} + Z_{sp} + Z_A \quad (1)$$

The angles α_2 and β_1 are flow angles. The inflow angle α_2 to the runner can be determined from the guide wheel or volute geometry. The angle β_1 of the fluid exiting from the runner, which can be estimated from the throat area, differs from the blade angle β_{1B} because a vane-congruent flow cannot be expected in turbine operation. The hydraulic losses between the suction and discharge nozzles occur in the inlet casing (Z_E), in the impellers (Z_{La}), in the diffusers (Z_{Le}), in the volutes (Z_{sp}), and in the outlet casing (Z_A). Then, the PAT’s hydraulic efficiency η_h can be calculated as the ratio of theoretical head to actual head.

The power P_T available at the coupling of the turbine is smaller than the supplied power $\rho g H Q$, because of power losses. The power balance of a PAT can be thus expressed according to Equation (2):

$$P_T = \rho g H \eta_h (Q - Q_{sp} - Q_E) - P_m - \sum_1^{N_{st}} P_{RR} - \sum_1^{N_{st}} P_{S3} - P_{er} \quad (2)$$

where η_h is the hydraulic efficiency, Q is the useful flow rate, Q_{sp} is the leakage through the annular seal at the impeller inlet, Q_E is the leakage through the device for axial thrust balancing, P_m accounts for mechanical losses, P_{RR} represents disk friction losses, P_{S3} are throttling losses, and P_{er} accounts for friction losses created by the components of axial thrust balance devices.

The PAT's overall efficiency η_T at the coupling is given by Equation (3):

$$\eta_T = \frac{P}{\rho g H Q} \quad (3)$$

According to the methodology outlined in [29] and adapted by the same authors in [28], twenty-four parameters have to be set for tuning the simulation model on a given pump/PAT. Fourteen parameters are specific to the pump and deal with (i) geometric characteristics; (ii) flow and geometrical angles, and (iii) hydraulic and power losses. These parameters may be known from pump geometry or can be estimated through an optimization procedure as made in [28]. Nine out of fourteen pump parameters are also required for the setup of the PAT model. Moreover, ten additional parameters are required for tuning the simulation model on the corresponding PAT: two parameters allow the identification of the BEP of the PAT, three parameters refer to hydraulic losses, while the remaining five parameters are used to tune power losses and thus estimate the useful power.

An optimization algorithm was used in [28] to identify the optimal value of model parameters. First, the simulation model was tuned in order to simulate pump behavior. Then, by using nine pump parameters, the same optimization algorithm was also used to identify the optimal parameter values for reproducing PAT performance.

2.2. Derakhshan and Nourbakhsh's Model

This Section presents the gray box model developed by Derakhshan and Nourbakhsh in [16], hereafter called "DN model". This model makes use of relations to predict the BEP of a pump working as a turbine, based on pump hydraulic characteristics. Moreover, two equations are used to estimate the complete characteristic curves of centrifugal PATs based on their BEP.

The first step of this methodology consists of the prediction of the BEP of a PAT. To this purpose, four nondimensional parameters for flow rate, head, power and efficiency are defined, as the ratio of the quantity at the BEP of a PAT to the same quantity at the BEP of the corresponding pump. Therefore, some relations, which also account for pump and PAT nondimensional specific speeds, can be obtained to calculate the BEP of the PAT based on the BEP of the pump, as shown by the functional dependencies expressed in Equations (4) and (5):

$$\psi_{BEP,T} = f_{DN1}(\Omega_P, \Omega_T, \phi_{BEP,P}, \phi_{BEP,T}, \psi_{BEP,P}) \quad (4)$$

$$P_{BEP,T} = f_{DN2}(\Omega_P, \Omega_T, \psi_{BEP,P}, \psi_{BEP,T}, P_{BEP,P}) \quad (5)$$

Equations (4) and (5) are disclosed in [16] and are valid for low-specific-speed centrifugal pumps.

The second step consists of the estimation of the complete performance curve of head and power. In [16], the nondimensional head is expressed as a function of nondimensional flow rate by means of a second order polynomial, as shown in Equation (6):

$$\frac{\psi_T}{\psi_{BEP,T}} = b_{DN1} \left(\frac{\phi_T}{\phi_{BEP,T}} \right)^2 + b_{DN2} \left(\frac{\phi_T}{\phi_{BEP,T}} \right) + b_{DN3} \quad (6)$$

Similarly, the nondimensional power is expressed as a function of nondimensional flow rate by means of a *third* order polynomial, as shown in Equation (7):

$$\frac{P_T}{P_{BEP,T}} = b_{DN4} \left(\frac{\phi_T}{\phi_{BEP,T}} \right)^3 + b_{DN5} \left(\frac{\phi_T}{\phi_{BEP,T}} \right)^2 + b_{DN6} \left(\frac{\phi_T}{\phi_{BEP,T}} \right) + b_{DN7} \quad (7)$$

Experimental data in [16] showed that the dimensionless characteristic curves of all PATs based on their BEP were approximately the same. The efficiency curve can be obtained by using its definition (i.e., Equation (3)), on the basis of the corresponding values of head and power.

2.3. Singh and Nestmann's Model

This section presents the gray box prediction model of Singh and Nestmann (hereafter called "SN model"), developed in [30,31] by using proprietary field data. The prediction model only requires the pump shape and size as input parameters and it is composed of four steps.

Step #1. To initiate the application of the prediction model, a link between pump and PAT specific speed has to be identified. In literature, such a relationship is usually found out to be linear, as shown in Equation (8).

$$\Omega_T = b_{SN1} \Omega_P + b_{SN2} \quad (8)$$

Step #2. It is known that PAT best efficiency points can be plotted on a Cordier diagram format and the mean Cordier PAT line provides a relationship between turbine specific speed and turbine specific diameter, according to Equation (9).

$$\Omega_T = f_{SN1}(\phi_T, \psi_T) \quad (9)$$

Therefore, the respective head and discharge values can be estimated at the BEP for any given point on the mean Cordier PAT line. The magnitude of the BEP of a given PAT can be determined by using efficiency scaling laws.

Step #3. The nondimensional head number and efficiency characteristics have to be used to identify the no-load points; in fact, there is a unique relationship between nondimensional head and nondimensional flow at no load, as shown in Equation (10).

$$\psi_{n1,T} = b_{SN3}(\phi_{n1,T})^{b_{SN4}} \quad (10)$$

Step #4. Head and efficiency curves are predicted in [31] via the Hermite spline approach. This method makes use of two fixed points on the curves (i.e., BEP and no-load point) and the slopes at these points to define a three-degree polynomial for the respective characteristics. In this manner, both the mean value and the uncertainty bands can be predicted for head and efficiency for a given pump specific speed.

Finally, it is worth noting that Singh and Nestmann identify two sources of error in their formulation, i.e., experimental and external errors. These errors depend on the accuracy that can be achieved in the determination of pump BEP, pump specific speed, and manufacturing tolerances. In [31], the authors provide an estimate of the uncertainties only at the BEP, in the range from approximately 5% at high rotational speed to approximately 15% at low rotational speed.

2.4. Evolutionary Polynomial Regression Model

Evolutionary Polynomial Regression (EPR) is a data-driven black box modelling technique based on genetic programming and numerical regression [32]. From a system identification perspective, EPR can be considered as a nonlinear global stepwise regression approach providing symbolic formulation for models. This technique has been developed and applied in several frameworks in recent years [33–35]. Some interesting and useful properties of EPR are related to the possibility of

(1) introducing existing prior knowledge on the considered phenomenon and (2) selecting the most effective model according to modelling purpose.

The general expression of the EPR formula is given as:

$$o = \sum_{i=1}^{N_t} F(\mathbf{p}, f(\mathbf{p}), c_i) + c_0 \quad (11)$$

where o is the estimated output of the process, F is the function identified through an evolutionary searching strategy, \mathbf{p} is the vector of input variables (made up of N_p elements), c_i is a constant value, f is a function defined by the user (such as natural logarithm, exponential, etc.), and N_t is the length (number of terms) of the polynomial (bias c_0 excluded, if any) [32].

Thanks to this general formula, EPR allows the use of several pseudo polynomial expressions belonging to the class of Equation (11). In particular, a sample expression of the function, which avoids the use of trigonometric functions or natural logarithm, is reported in Equation (12):

$$o = c_0 + \sum_{i=1}^{N_t} c_i p_1^{\gamma_{i,1}} p_2^{\gamma_{i,2}} \dots p_{N_p}^{\gamma_{i,N_p}} \quad (12)$$

Equation (12) can be used when output is not characterized by periodicity, as in the case considered in this study.

The actual form of Equation (12) is identified through an evolutionary searching strategy where the decision variables are the inputs p_1, p_2, \dots, p_{N_p} to be considered in each monomial of the summation and the corresponding exponents $\gamma_1, \gamma_2, \dots, \gamma_{N_p}$ while the coefficients c_0 and c_i (with $i = 1:N_t$) are estimated through numerical regression in order to minimize the sum of the square errors [32].

The optimal solution identified by the EPR algorithm with respect to the data considered in this paper (see Section 3.1) is reported in Equations (13)–(15) for nondimensional head, nondimensional power, and efficiency, respectively.

$$\begin{aligned} \psi_T = & b_{EPR1}\Omega^{-5} + b_{EPR2}\Omega^{-1} + b_{EPR3}\phi\Omega^{-12} + b_{EPR4}\phi + b_{EPR5}\phi\Omega^2 + b_{EPR6}\phi^2\Omega^{-12} + b_{EPR7}\phi^2\Omega^{-7} + \\ & + b_{EPR8}\phi^2 + b_{EPR9}\phi^3\Omega^{-4} + b_{EPR10}\phi^4\Omega^{-2} + b_{EPR11}\phi^4\Omega^{-1} + b_{EPR12}\phi^4\Omega + b_{EPR13}\phi^5\Omega^{-10} + \\ & + b_{EPR14}\phi^5\Omega^{-17} + b_{EPR15}\phi^6\Omega^{-6} + b_{EPR16}\phi^8\Omega^8 + b_{EPR17}\phi^{10} + b_{EPR18}\phi^{12} + b_{EPR19}\phi^{14}\Omega^{14} + b_{EPR20} \end{aligned} \quad (13)$$

$$\begin{aligned} \pi_T = & b_{EPR21}\phi^{-2}\Omega^{-20} + b_{EPR22}\phi^{-2} + b_{EPR23}\phi^{-1}\Omega^{-7} + b_{EPR24}\phi^{-1} + b_{EPR25}\phi^{-1}\Omega^9 + b_{EPR26}\Omega^{-1} + \\ & + b_{EPR27}\Omega + b_{EPR28}\phi + b_{EPR29}\phi\Omega^5 + b_{EPR30}\phi\Omega^{12} + b_{EPR31}\phi^2\Omega^{-2} + b_{EPR32}\phi^2\Omega^2 + b_{EPR33}\phi^3\Omega^{-2} + \\ & + b_{EPR34}\phi^3\Omega^4 + b_{EPR35}\phi^5 + b_{EPR36}\phi^6\Omega + b_{EPR37}\phi^7\Omega + b_{EPR38}\phi^{10}\Omega^{18} + b_{EPR39} \end{aligned} \quad (14)$$

$$\begin{aligned} \eta_T = & b_{EPR40}\phi^{-4}\Omega^{-6} + b_{EPR41}\phi^{-3}\Omega^{-2} + b_{EPR42}\phi^{-3}\Omega^3 + b_{EPR43}\phi^{-2} + b_{EPR44}\phi^{-2}\Omega^2 + b_{EPR45}\phi^{-1}\Omega^2 + \\ & + b_{EPR46}\phi^{-1}\Omega^3 + b_{EPR47}\Omega + b_{EPR48}\Omega^2 + b_{EPR49}\phi\Omega^{-1} + b_{EPR50}\phi + b_{EPR51}\phi\Omega + b_{EPR52}\phi^2\Omega^{-12} + \\ & + b_{EPR53}\phi^2 + b_{EPR54}\phi^3\Omega^{-1} + b_{EPR55}\phi^4\Omega^{-4} + b_{EPR56}\phi^4\Omega^{12} + b_{EPR57}\phi^6\Omega + b_{EPR58}\phi^7 + b_{EPR59}\phi^9\Omega + b_{EPR60} \end{aligned} \quad (15)$$

To improve data fitting, the EPR solver was allowed to search a functional dependency composed of up to 20 terms (actually, all Equations (13)–(15) are composed of 20 terms) and the searching space for exponents was set in the range from -20 to $+20$ to consider a high number of polynomial expressions (in fact, no exponent is equal to -20 or $+20$).

The interpolating functions expressed in Equations (13)–(15) are difficult to interpret from a physical point of view, since they were mainly aimed at fitting the available experimental data in the best possible way. At the same time, they clearly highlight the complexity of relating PAT performance curves to pump performance curves.

3. Pump and Pumps as Turbines Data

3.1. Available Field Data from Literature

The available data for testing the four approaches are the ones reported in [16] by Derakhshan and Nourbakhsh, who also developed the DN model outlined in Section 2.2. In fact, in [16] the authors documented the experimental performance curves of four pumps/PATs over the entire range of operation. The specific speed of the four pumps ranges from 1.53 to 5.82.

The pump characteristic values at the respective BEP are reported in Table 1. As also made in [8], the experimental nondimensional data reported in [16] were rendered dimensional by considering n equal to 25 rps (i.e., 1500 rpm) and pump nominal diameter D equal to 0.25 m. Therefore, the values in Table 2 represent the experimental BEP, documented by the measured values reported in [16].

Table 1 highlights that the volume flow rate at BEP covers the range from 8.0 L/s to 107.7 L/s, BEP power ranges from about 3 kW to about 22 kW, while BEP efficiency passes from 64.5% to 86.8%. The head at BEP passes from 24.9 m (pump #1) to 18.3 m (pump #4).

Table 2 reports the operating ranges of the four pumps/PATs. For a given PAT, the range of variation of the volume flow rate of head, power, and efficiency is almost the same. Instead, for a given pump, the range of variation of the volume flow rate of head, power, and efficiency can be quite different, mainly the lower bound. As can be noticed, the highest flow rate swallowed by pump #4 is 148 L/s, the maximum head is 29 m (pump #1), while maximum values of power and efficiency are about 25 kW and 87%, respectively (both values refer to pump #4). Instead, the highest flow rate swallowed by a PAT (PAT #4) is 129 L/s, i.e., it is slightly lower than that of the pump #4. The range of variation of PAT head strongly depends on the considered PAT, e.g., it is in the range 27 m–68 m for PAT #1 and 12 m–27 m for PAT #4. The maximum producible electric power is in agreement with the corresponding pump value (i.e., less than 5 kW for PAT #1 up to more than 25 kW for PAT #4). Finally, for a given pump, the maximum value of pump efficiency is higher than the maximum value of the corresponding PAT.

Table 1. Pump characteristics at Best Efficiency Point (BEP) [16].

Pump	Ω , -	Q , 10^{-3} m ³ /s	η , %	H , m	P , W
#1	1.53	8.0	64.5	24.9	3044
#2	2.41	24.8	75.7	22.1	7114
#3	3.94	62.2	86.3	21.1	14,926
#4	5.82	107.7	86.8	18.3	22,288

Table 2. Pump and pumps as turbines (PAT) operating range reported in [16].

Pump	#1	#2	#3	#4
Q , 10^{-3} m ³ /s	0.0–12.7	0.0–43.9	0.0–94.4	0.0–148.3
H , m	15.3–29.2	10.9–24.7	12.5–25.5	12.4–23.1
Q , 10^{-3} m ³ /s	2.0–6.6	6.6–43.5	16.9–95.5	28.5–148.0
P , W	1559–2525	4084–9504	8465–18,860	14,405–24,800
Q , 10^{-3} m ³ /s	2.5–12.7	4.9–43.7	8.7–94.7	16.4–146.1
η , %	40.1–64.5	30.0–75.7	30.3–86.3	30.0–86.8
PAT	#1	#2	#3	#4
Q , 10^{-3} m ³ /s	10.4–18.3	19.5–43.5	31.5–95.9	55.2–129.3
H , m	27.0–67.7	19.8–50.8	15.4–38.7	12.1–27.1
Q , 10^{-3} m ³ /s	10.3–18.6	19.2–44.5	31.8–95.9	55.1–131.7
P , W	668–4752	817–15,296	0–26,582	0–25,468
Q , 10^{-3} m ³ /s	10.1–18.5	18.5–44.0	32.2–96.1	53.8–130.7
η , %	24.8–63.1	25.1–71.6	0.0–74.7	0.0–78.3

3.2. Pump and Pumps as Turbines (PAT) Performance Curves

In this work, pump and PAT experimental characteristic curves described in [16] are modeled independently. In fact, the authors found out in [8] that second-order polynomials guarantee the best fit for all the nondimensional parameters Y , for both the pump and the PAT, as described by Equations (16) and (17), respectively. In this manner, the trend over the entire range of operation can also be reproduced in a physically consistent way.

$$Y_P(\Omega, \phi) = a_{2P}(\Omega) \cdot \phi^2 + a_{1P}(\Omega) \cdot \phi + a_{0P}(\Omega) \quad (16)$$

$$Y_{PAT}(\Omega, \phi) = a_{2T}(\Omega) \cdot \phi^2 + a_{1T}(\Omega) \cdot \phi + a_{0T}(\Omega) \quad (17)$$

The modeling approach expressed in Equations (16) and (17) is shown in Figure 1, which is derived from [8]. For the sake of comparison, both pump and PAT flow rate is assumed positive. As discussed in [8], the agreement between experimental data and interpolation curves of head is very good in both pump and PAT mode (in the range 0.5–2.6%), while the deviation is slightly higher for power curves of PATs (values in the range 1.9–7.5%). Therefore, this also reflects on efficiency curves. However, it should be noted that, according to [16], the uncertainty of the experimental data of head, flow rate, power, and efficiency were $\pm 5.5\%$, $\pm 3.4\%$, $\pm 5.1\%$, and $\pm 5.5\%$, respectively. Therefore, the modeling approach represented by Equations (16) and (17) can be judged suitable for the purpose of this paper, as the trend of pump and PAT performance curves is physics-responding over the entire range of operation.

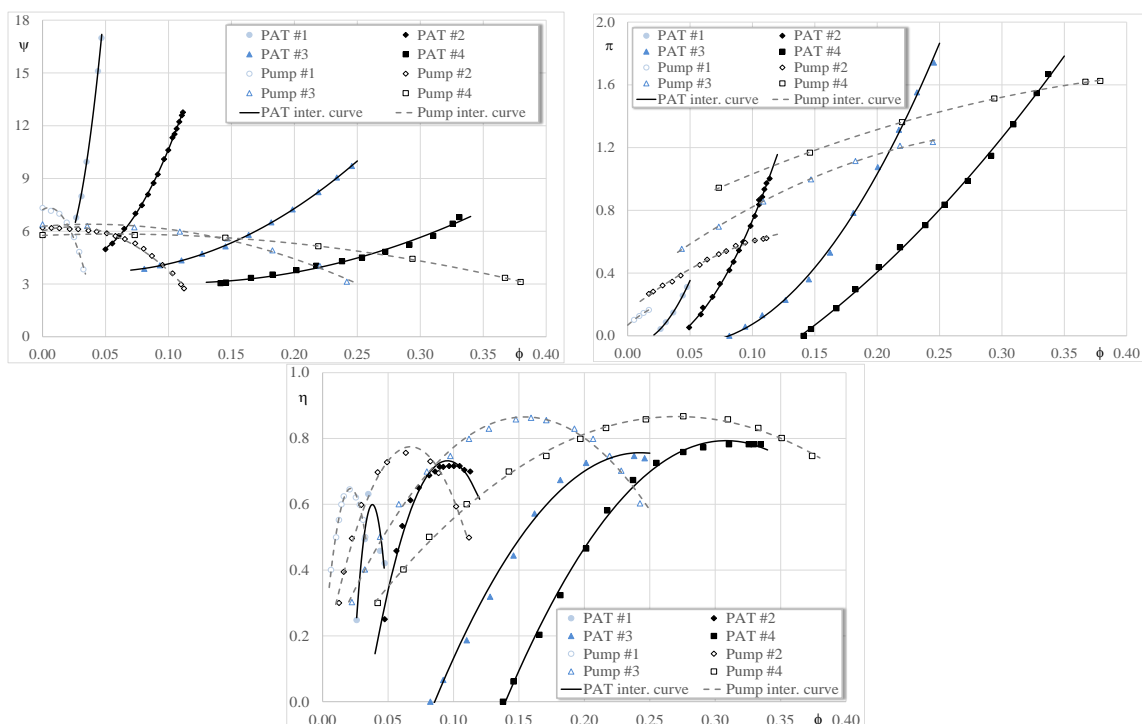


Figure 1. Nondimensional head, nondimensional power, and efficiency vs. nondimensional flow rate (symbols: experimental data [16]; lines: interpolation curves [8]).

4. Results

4.1. Performance Curves

The values predicted by the four approaches (PB, DN, SN, and EPR), compared to the original field data taken from [16], are reported in Figures 2–4 for nondimensional head, nondimensional power, and efficiency, respectively. It can be observed that:

- in general, the values predicted by all the four models are in agreement with the field data trend and the predicted trend is all in all physically sound over the entire range of operation;
- head is reproduced well by all models, mainly at higher flow rates and mainly for PAT #4. Instead, the accuracy of PAT #1 predicted by the SN model is poor;
- power is also qualitatively predicted by all models in a physically consistent way, with the exception of the SN model. In fact, SN model predictions considerably differ from the experimental values and some predictions for PAT #1 and PAT #2 are even lower than zero. In general, the trend of predicted PATs progressively departs from the experimental data by increasing the specific speed (i.e., by passing from PAT #1 to PAT #4);
- as a consequence of the comments about head and power, efficiency values predicted by the four models are much more scattered, in particular the ones predicted by the SN model. In general, they also deviate from experimental data in correspondence of the respective BEP. PAT #3 is most accurately reproduced by all models.

However, it should be remarked that the SN model was developed in [31] on different data than the ones considered in this paper; in particular, the data used in [31] were characterized by higher specific speeds (in the range 3.81–9.89).

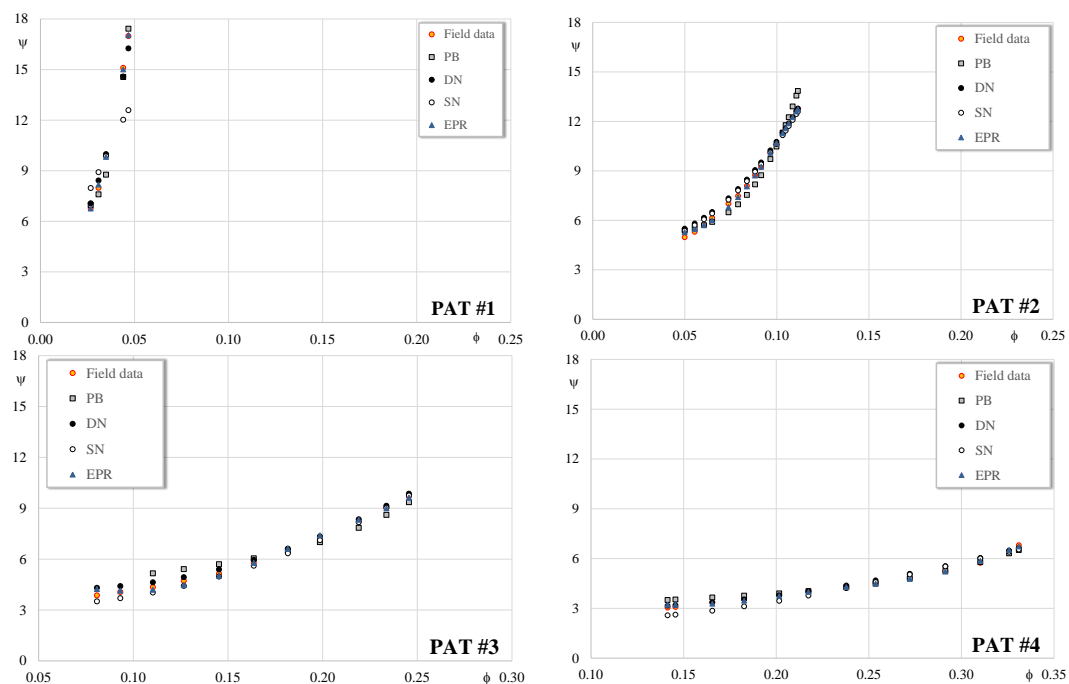


Figure 2. Nondimensional head vs. nondimensional volume flow rate.

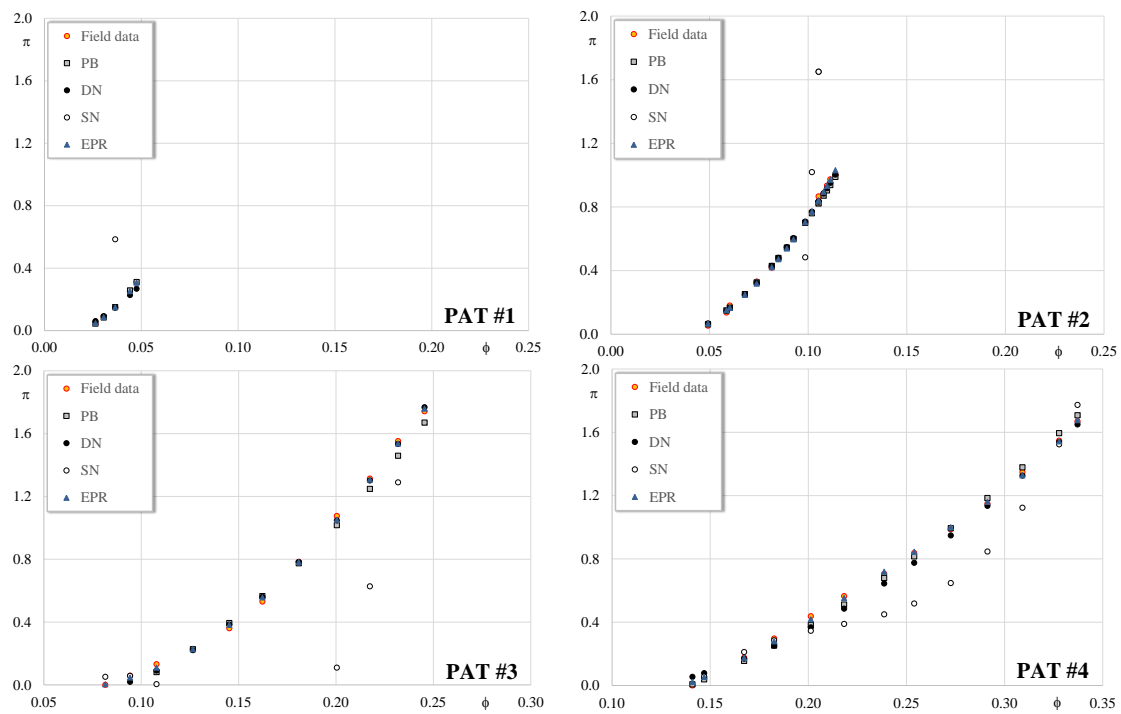


Figure 3. Nondimensional power vs. nondimensional volume flow rate.

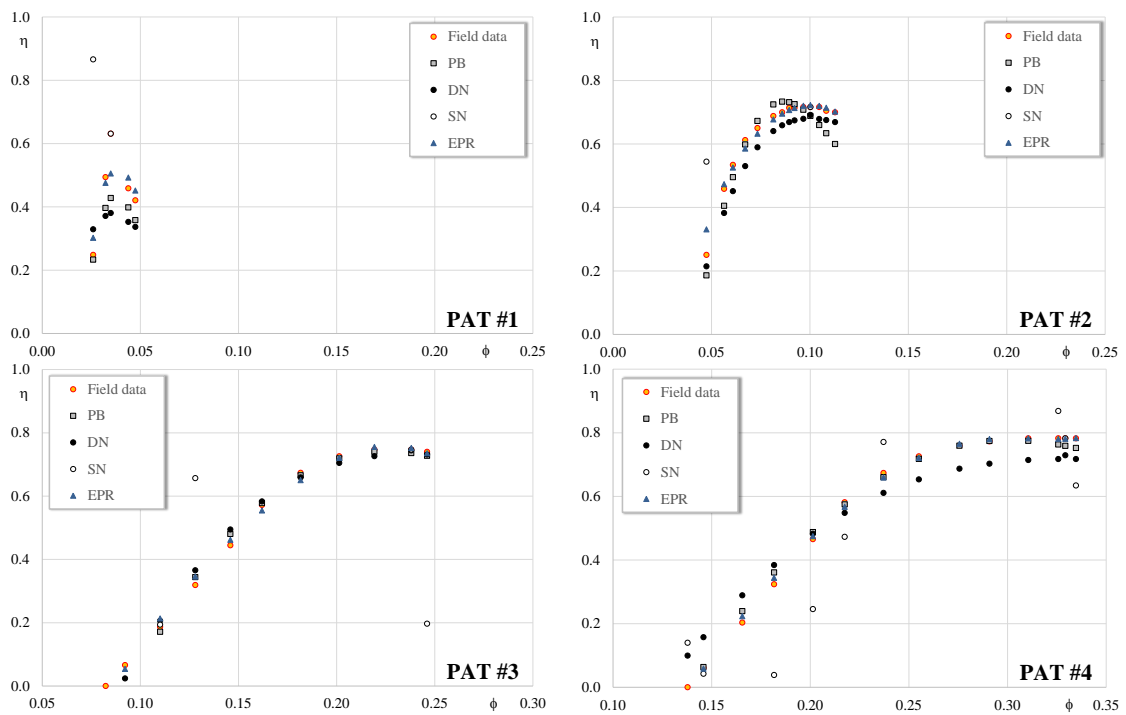


Figure 4. Efficiency vs. nondimensional volume flow rate.

4.2. Reliability

In this section, the reliability of PAT curve prediction is assessed, with respect to the field data reported in [16]. To this aim, the root mean square relative error $RMSE_{Y_k}$, defined in Equation (18) is adopted:

$$RMSE_{Y_k} = \sqrt{\frac{1}{N_e} \sum_{i=1}^{N_e} \left(\frac{(Y_{ki})_e - (Y_{ki})_s}{(Y_{ki})_e} \right)^2} \quad Y = \psi, \pi, \eta; k = 1, 2, 3, 4 \quad (18)$$

The $RMSE_{Y_k}$ compares the experimental values reported in [16] of the performance parameter $(Y_{ki})_e$ for a given PAT k to the corresponding simulated value $(Y_{ki})_s$, predicted by means of the four models.

However, it is worth noting that the prediction errors over the entire range of operation were not reported in [16]. Moreover, in this paper, the operating points at the lowest φ were not considered for calculating root mean square relative error (RMSE) for PAT #3 and #4, since both power and efficiency were equal to zero.

The values of $RMSE_{Y_k}$ are summarized in Figures 5–7 for nondimensional head, nondimensional power, and efficiency, respectively. In agreement with the comments made on the performance curve trends, it can be highlighted that:

- in general, the RMSE of nondimensional head is quite acceptable for all models. In fact, the overall RMSE is equal to 6.9% for the PB model, 4.0% for the DN model, 8.1% for the SN model, and 2.1% for the EPR model. Only one large value of RMSE (i.e., 17.5%) is calculated by the SN model for PAT #1;
- RMSE values of nondimensional power are in general higher (in some cases considerably higher) than the corresponding values for nondimensional head. Moreover, each modeling approach follows a different scheme to reproduce the different PATs. With regard to the PB model, the RMSE of power is roughly comparable to the RMSE of head (the maximum value is 13.8% for PAT #3). The DN model predicts well the PAT #2 and PAT #3 (RMSE equal to 7.3% and 10.7%), while the RMSE for PAT #1 and PAT #4 are high (19.7% and 23.8%). The predictions made by the SN model are unacceptable for all PATs, even though they tend to decrease by increasing the specific speed. Finally, the EPR model predicts well all PATs (maximum RMSE equal to 6.8%);
- as a consequence of the combined effect of RMSE values of head and power, the RMSE values of efficiency are, in some cases, high. In fact, the reliability of PB model prediction ranges from 4.8% to 19.3%. As already observed for power, the DN model predicts well PAT #2 and PAT #3 (RMSE equal to 3.5% and 8.8%). The efficiency estimated by the SN model is poorly predicted for all PATs. Finally, RMSE values obtained by using the EPR model may be all in all acceptable (the maximum value is equal to 14.1% for PAT #1) and decrease by increasing the specific speed.
- As a final remark, it should be observed that the fact that PAT performance can be sometimes predicted with large errors is confirmed by the results presented in [23], where, as made in this paper, several methodologies were compared. For the majority of the models analyzed in [23], the head and flow at BEP had errors above 10%; in some cases, errors were approximately 20% and in a few cases they were higher than 80%.

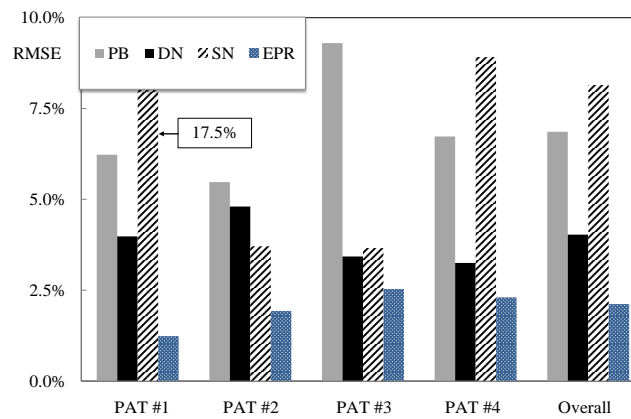


Figure 5. RMSE for nondimensional head.

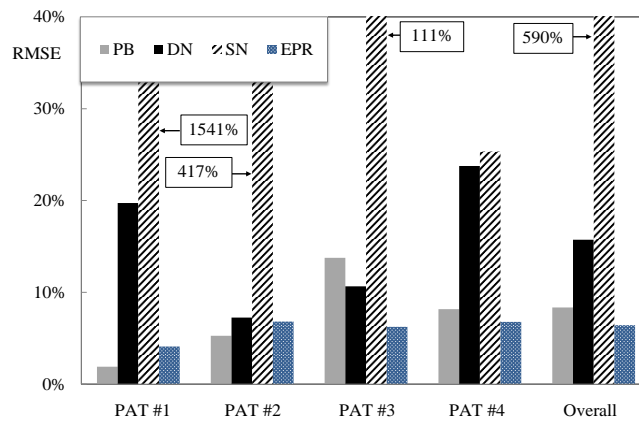


Figure 6. RMSE for nondimensional power.

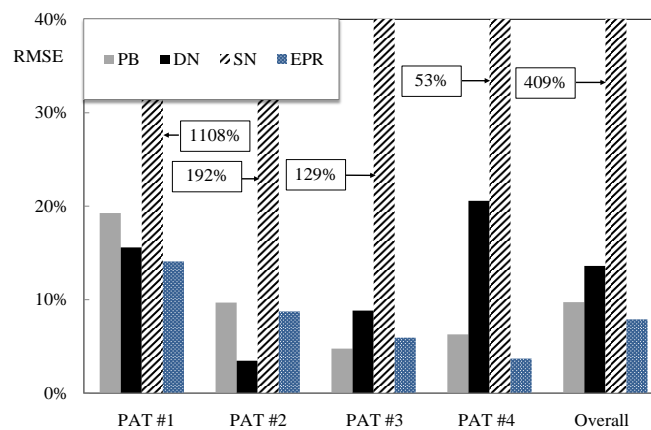


Figure 7. RMSE for efficiency.

4.3. Discussion

In the framework of the results presented in Sections 4.1 and 4.2, some general remarks can be made to highlight advantages and drawbacks of each approach.

As a general comment, it has to be observed that the values of both nondimensional power and efficiency at the lowest flow rates of each specific speed are very close to zero and therefore, even though the absolute deviation between model prediction and experimental value may be low as

shown in Figures 3 and 4, the relative deviation may be huge. In fact, as highlighted in Section 4.1, the trend of power and efficiency is predicted in a physical-consistent way.

Moreover, it has to be highlighted that the prediction errors of the DN model over the entire range of operation were not reported in the paper [16], though both the experimental data and the model were presented. In [16], Derakhshan and Nourbakhsh only documented the values of the ratio of PAT head at BEP to pump head at BEP ($\psi_{\text{BEP,T}}/\psi_{\text{BEP,P}}$) for their own method and for three other methods reported in literature. The DN model is characterized by a relative deviation at BEP in the range from -4.4% to 4.6% , while the relative deviation at BEP of the other methods varies in the range from -7.30% to 28.3% . Moreover, the results documented in [20] showed the validity of the power curve equation provided by Derakhshan and Nourbakhsh [16] only for low flow rates, while both the head curve and the proposed equation for the horizontal pump studied in [20] underestimated experiments up to 30% .

Singh and Nestmann also did not report in [31] the prediction errors of their own model over the entire range of operation. As recalled in Section 2.3, uncertainty values of head at BEP range from approximately 5% at high rotational speed to approximately 15% at low rotational speed. However, the modeling approach adopted in [31] was considered accurate enough for the purpose of that paper, i.e., the selection of the most suitable pump available in the market for two installations. It should also be highlighted that the PATs considered in [31] are characterized by specific speed values in the range $3.81\text{--}9.89$, while the PATs considered in this paper have specific speeds in the range $1.53\text{--}5.82$. In fact, the SN model most poorly predicts the performance of PAT #1 and PAT #2.

Instead, the prediction error of the EPR model at BEP is usually very low (in the range from -2.1% to 1.5%), with the exception of the efficiency of PAT #1, for which the prediction error at BEP is equal to 19.9% (see Figure 4 for PAT #1). In fact, the EPR model is suitable for data fitting purposes.

Finally, it has to be noted that, while the PB, the DN, and the SN models estimate PAT efficiency according to Equation (3) and therefore head, power, and efficiency are always consistent, the EPR model developed in this paper makes use of an independent expression tuned on the available data (i.e., Equation (15)). However, it was verified that the application of Equation (3) for estimating a PAT's efficiency on the basis of the PAT's head and power predicted by the EPR model through Equations (13) and (14) leads to higher prediction errors (up to 22%) than the ones obtained by using Equation (15) and reported in Figure 7. This finding highlights that it is preferable to fit the available data by means of the EPR model instead of propagating prediction errors on head and power by using Equation (3) to estimate PAT efficiency.

Therefore, the lessons learnt from the analyses carried out in this paper can be summarized as follows:

- the PB model proves to be the best approach, since it is general and sufficiently accurate. However, (i) PB model development requires detailed insight into pump and PAT operation and (ii) model tuning may be challenging, as the order of magnitude of several parameters have to be known a priori on the basis of engineering practice;
- the DN model is intuitive, physically sound, and easy to apply. However, though this method is tested in this paper against the same data used by Derakhshan and Nourbakhsh to develop their own model, the RMSE values over the entire range of operation can be sometimes high, mainly for power and efficiency;
- the SN model, characterized by a similar approach to that of the DN model (so, it is physically sound and easy to apply as well), proves to be the least accurate among the considered approaches. However, this method was developed by Singh and Nestmann by considering higher specific speeds ($3.81\text{--}9.89$) than the ones characterizing the experimental data considered in this paper ($1.53\text{--}5.82$).
- the EPR model is always better than the PB model for predicting head and, in some cases, it is also better for predicting power and efficiency. However, by nature, a black box model is specific to its training data, which must also include PAT performance. In fact, the well-known limit of

such a modeling approach is high prediction errors when black box models operate outside the field in which they were trained. Therefore, great attention has to be paid to proper selection of training data. This approach was considered in this paper to highlight that, even though a complex and high-degree polynomial is adopted, prediction errors may be high (14.1% in the worst case). Therefore, a simpler polynomial with a lower degree (i.e., an underparameterized model), which may allow more intuitive physical interpretation, would lead to even higher prediction errors.

In summary, even though its development may be time consuming, the physics-based model developed in [28] represents a powerful tool for estimating PAT performance curves over the entire range of operation on the basis of pump characteristics, since (i) published data of the performance curves of pumps running in reverse mode are limited; (ii) no single modeling approach available in literature reproduces the experimental behavior of PATs throughout the whole range of operation, and (iii) other competitive approaches such as black box models, even though they may allow lower prediction errors, may be characterized by significant drawbacks, e.g., specificity of model application.

5. Conclusions

In this paper, four approaches (one physics-based simulation model, two “gray box” models, and one “black box” model) suitable for the reconstruction of PAT performance curves were analyzed. The considered methodologies were applied to the experimental data of four pumps/PATs, having a specific speed in the range 1.53–5.82. The results presented in this paper show that:

- in general, the values predicted by all the four models are in agreement with the field data trend, which is all in all physically sound over the entire range of operation. Head and power are reproduced well by all models mainly at higher flow rates, while efficiency values predicted by the four models are considerably scattered, in particular the ones predicted by the model developed by Singh and Nestmann;
- the overall RMSE of nondimensional head is quite acceptable for all models (from 2.1% to 8.1%), while the overall RMSE values of nondimensional power and efficiency are in general higher.

In summary, the black box model (EPR) proves to be the most accurate approach, followed by the physics-based model and the gray box model developed by Derakhshan and Nourbakhsh. However, black box models require the availability of input/output data for their setup, which is therefore specific to a given fleet of machines. Even though physics-based model development requires detailed insight into pump and PAT operation and model tuning may be challenging, the physics-based model may represent a more general tool to also reproduce PATs not previously considered for model tuning.

Acknowledgments: This study was carried out within the research project “ERC (Energy Recovery in Cities)—Studio di tecnologie innovative per il recupero di energia residuale in ambiente urbano” in the framework of the “Bando 2016 per progetti di ricerca finanziati con il contributo della Camera di Commercio, Industria, Artigianato e Agricoltura”.

Author Contributions: Mauro Venturini, Stefano Alvisi, Silvio Simani and Lucrezia Manservigi conceived and designed the study; Mauro Venturini, Stefano Alvisi, Silvio Simani and Lucrezia Manservigi performed the study; Mauro Venturini, Stefano Alvisi, Silvio Simani and Lucrezia Manservigi analyzed the data; Mauro Venturini, Stefano Alvisi, Silvio Simani and Lucrezia Manservigi wrote the paper.

Conflicts of Interest: The authors declare no conflict of interest.

Nomenclature

a	interpolation curve coefficient, -
b	parameter in DN and SN model, -
BEP	best efficiency point
c	absolute velocity, m/s
c_i	constant of EPR model, -
D	pump nominal diameter, m
DN	Derakhshan and Nourbakhsh's model
EPR	Evolutionary Polynomial Regression model
f/F	function of EPR model, -
g	gravitational acceleration, m/s ²
H	head, m
k	index of pump/PAT ($k = 1,2,3,4$), -
n	rotational speed, rps
N	number, -
o	output of EPR model, -
\mathbf{p}	vector of input variables of the EPR model, -
P	power, W
PB	physics-based model
PAT	pump as turbine
Q	volume flow rate, m ³ /s
RMSE	root mean square relative error, -
SN	Singh and Nestmann's model
u	circumferential velocity, m/s
Υ	nondimensional performance parameter (π, η, ψ), -
Z	hydraulic loss, m

Greek symbols

α	angle between direction of circumferential and absolute velocity
β	angle between relative velocity vector and the negative direction of circumferential velocity
φ	nondimensional volume flow rate defined as $Q/(nD^3)$, -
γ	exponent of the EPR model, -
η	efficiency, -
π	nondimensional power defined as $P/(\rho n^3 D^5)$, -
ρ	density, kg/m ³
ψ	nondimensional head defined as $gH/(n^2 D^2)$, -
ω	angular velocity, rad/s
Ω	specific speed defined as $\omega \cdot Q^{0.5} / (gH)^{0.75}$, -

Subscripts and superscripts

A	outlet casing
B	blade
BEP	best efficiency point
DN	Derakhshan and Nourbakhsh's model
e	experimental
E	inlet casing
EPR	Evolutionary Polynomial Regression model
er	friction created by the components of axial thrust balance devices
h	hydraulic
La	impeller
Le	diffuser
m	mechanical, meridional component
nl	no-load condition in SN model
p	input variable of the EPR model

P	pump
RR	disk friction
s	simulated
s3	throttling
SN	Singh and Nestmann's model
sp	volute
t	terms in the EPR model
T	PAT
Y	nondimensional parameter

References

1. Carravetta, A.; Del Giudice, G.; Fecarotta, O.; Ramos, H. Energy Production in Water Distribution Networks: A PAT Design Strategy. *Water Resour. Manag.* **2012**, *26*, 3947–3959. [[CrossRef](#)]
2. Zakkour, P.; Gochin, R.; Lester, J. Developing a sustainable energy strategy for a water utility. Part II: A review of potential technologies and approaches. *Environ. Manag.* **2002**, *66*, 115–125. [[CrossRef](#)]
3. Sammartano, V.; Arico, C.; Carravetta, A.; Fecarotta, O.; Tucciarelli, T. Banki-michell optimal design by computational fluid dynamics testing and hydrodynamic analysis. *Energies* **2013**, *6*, 2362–2385. [[CrossRef](#)]
4. Ramos, H.; Borga, A. Pump as turbine: An unconventional solution to energy production. *Urban Water* **1999**, *1*, 261–263. [[CrossRef](#)]
5. Jain, S.V.; Patel, R.N. Investigations on pump running in turbine mode: A review of the state-of-the-art. *Renew. Sustain. Energy Rev.* **2014**, *30*, 841–868. [[CrossRef](#)]
6. Carravetta, A.; Antipodi, L.; Golia, U.; Fecarotta, O. Energy saving in a water supply network by coupling a pump and a pump as turbine (PAT) in a turbopump. *Water* **2017**, *9*, 62. [[CrossRef](#)]
7. Sinagra, M.; Sammartano, V.; Morreale, G.; Tucciarelli, T. A new device for pressure control and energy recovery in water distribution networks. *Water* **2017**, *9*, 309. [[CrossRef](#)]
8. Venturini, M.; Alvisi, S.; Simani, S.; Manservigi, L. Energy potential of pumps as turbines (PATs) in water distribution networks. *Energies* **2017**, *10*, 1666. [[CrossRef](#)]
9. Carravetta, A.; Del Giudice, G.; Fecarotta, O.; Ramos, H.M. Pump as turbine (PAT) design in water distribution network by system effectiveness. *Water* **2013**, *5*, 1211–1225. [[CrossRef](#)]
10. Simani, S.; Alvisi, S.; Venturini, M. DataDriven Design of a Fault Tolerant Fuzzy Controller for a Simulated Hydroelectric System. In Proceedings of the 9th IFAC Symposium on Fault Detection, Supervision and Safety for Technical Processes, Paris, France, 2–4 September 2015; pp. 1090–1095.
11. Simani, S.; Alvisi, S.; Venturini, M. Fault Tolerant Control of a Simulated Hydroelectric System. *Control Eng. Pract.* **2016**, *51*, 13–25. [[CrossRef](#)]
12. Simani, S.; Alvisi, S.; Venturini, M. Fault Tolerant Model Predictive Control Applied to a Simulated Hydroelectric System. In Proceedings of the 3rd International Conference on Control and Fault-Tolerant Systems—SysTol'16, Barcelona, Spain, 7–9 September 2016; IEEE Control Systems Society, Ed.; pp. 251–256.
13. Finotti, S.; Simani, S.; Alvisi, S.; Venturini, M. Benchmarking of Advanced Control Strategies for a Simulated Hydroelectric System. In Proceedings of the 13th European Workshop on Advanced Control and Diagnosis (ACD 2016), Lille, France, 17–18 November 2016; pp. 1–12.
14. De Marchis, M.; Fontanazza, C.M.; Freni, G.; Messineo, A.; Milici, B.; Napoli, E.; Notaro, V.; Puleo, V.; Scopa, A. Energy recovery in water distribution networks. Implementation of pumps as turbine in a dynamic numerical model. *Procedia Eng.* **2014**, *70*, 439–448. [[CrossRef](#)]
15. De Marchis, M.; Milici, B.; Volpe, R.; Messineo, A. energy saving in water distribution network through pump as turbine generators: Economic and environmental analysis. *Energies* **2016**, *9*, 877. [[CrossRef](#)]
16. Derakhshan, S.; Nourbakhsh, A. Experimental Study of Characteristic Curves of Centrifugal Pumps Working As Turbines in Different Specific Speeds. *Exp. Therm. Fluid Sci.* **2008**, *32*, 800–807. [[CrossRef](#)]
17. Derakhshan, S.; Nourbakhsh, A. Theoretical, Numerical and Experimental Investigation of Centrifugal Pumps in Reverse Operation. *Exp. Therm. Fluid Sci.* **2008**, *32*, 1620–1627. [[CrossRef](#)]
18. Yang, S.; Derakhshan, S.; Kong, F. Theoretical, Numerical and Experimental Prediction of Pump as Turbine Performance. *Renew. Energy* **2012**, *48*, 507–513. [[CrossRef](#)]

19. Derakhshan, S.; Kasaeian, N. Optimization, Numerical, and Experimental Study of a Propeller Pump as Turbine. *Energy Resour. Technol.* **2014**, *136*, 012005. [[CrossRef](#)]
20. Pugliese, F.; De Paola, F.; Fontana, N.; Giugni, M.; Marini, G. Experimental characterization of two Pumps as Turbines for hydropower generation. *Renew. Energy* **2016**, *99*, 180–187. [[CrossRef](#)]
21. Barbarelli, S.; Amelio, M.; Florio, G. Predictive model estimating the performances of centrifugal pumps used as turbines. *Energy* **2016**, *107*, 103–121. [[CrossRef](#)]
22. Barbarelli, S.; Amelio, M.; Florio, G. Experimental activity at test rig validating correlations to select pumps running as turbines in microhydro plants. *Energy Convers. Manag.* **2017**, *149*, 781–797. [[CrossRef](#)]
23. Tan, X.; Engeda, A. Performance of centrifugal pumps running in reverse as turbine: Part II—Systematic specific speed and specific diameter based performance prediction. *Renew. Energy* **2016**, *99*, 188–197. [[CrossRef](#)]
24. Frosina, B.; Buono, D.; Senatore, A. A performance prediction method for pumps as turbines (PAT) using a computational fluid dynamics (CFD) modeling approach. *Energies* **2017**, *10*, 103. [[CrossRef](#)]
25. Akaike, H. A new look at the statistical model identification. *IEEE Trans. Autom. Control* **1974**, *19*, 716–723. [[CrossRef](#)]
26. Ljung, L. *System Identification—Theory for the User*, 2nd ed.; Prentice-Hall: Upper Saddle River, NJ, USA, 1999.
27. Sjöberg, J.; Zhang, Q.; Ljung, L.; Benveniste, A.; Delyon, B.; Glorennec, P.Y.; Hjalmarsson, H.; Juditsky, A. Nonlinear black-box modeling in system identification: A unified overview. *Automatica* **1995**, *31*, 1691–1724. [[CrossRef](#)]
28. Venturini, M.; Alvisi, S.; Simani, S.; Manservigi, L. Development of a Physics-Based Model to Predict the Performance of Pumps as Turbines (PATs). In Proceedings of the ECOS 2017, San Diego, CA, USA, 2–6 July 2017.
29. Gulich, J.F. *Centrifugal Pumps*, 3rd ed.; Springer: Berlin, Germany, 2010; ISBN 978-3-642-40113-8.
30. Singh, P.; Nestmann, F. An optimization routine on a prediction and selection model for the turbine operation of centrifugal pumps. *Exp. Therm. Fluid Sci.* **2010**, *34*, 152–164. [[CrossRef](#)]
31. Singh, P.; Nestmann, F. A Consolidated Model for the Turbine Operation of Centrifugal Pumps. *J. Eng. Gas Turbines Power* **2011**, *133*, 063002. [[CrossRef](#)]
32. Giustolisi, O.; Savic, D.A. A symbolic data-driven technique based on evolutionary polynomial regression. *J. Hydroinform.* **2006**, *8*, 207–222.
33. Giustolisi, O.; Savic, D.A. Advances in data-driven analyses and modelling using EPR-MOGA. *J. Hydroinform.* **2009**, *11*, 225–236. [[CrossRef](#)]
34. El-Baroudy, I.; Elshorbagy, A.; Carey, S.K.; Giustolisi, O.; Savic, D. Comparison of three Data-Driven Techniques in modelling the evapotranspiration process. *J. Hydroinform.* **2010**, *12*, 365–379. [[CrossRef](#)]
35. Alvisi, S.; Creaco, E.; Franchini, M. Crisp discharge forecasts and grey uncertainty bands using data-driven models. *Hydrol. Res.* **2012**, *43*, 589–602. [[CrossRef](#)]

